JOURNAL OF GEOPHYSICAL RESEARCH, VOL. 109, B05208, doi:10.1029/2004JB003027, 2004

Sliding of a rough surface under oblique loading

Joseph B. Walsh
Adamsville, Rhode Island, USA

Wenlu Zhu
Department of Geology and Geophysics, Woods Hole Oceanographic Institution, Woods Hole, Massachusetts, USA

Received 18 February 2004; accepted 25 March 2004; published 19 May 2004.

[1] Sliding of a rough surface having a range of asperity heights is a gradual process, starting at contacts under relatively low normal shear load and spreading until the surface slides as a unit. We analyze this process theoretically for asperities with spherical tips, with heights having a probability density distribution given by a negative exponential. The case where applied normal traction increases concurrently with applied shear is treated in detail, resulting in analytical expressions for the normal and shear displacements. These results are used to show limitations on constitutive behavior for more complex normal stress-shear stress histories. *INDEX TERMS:* 7209 Seismology: Earthquake dynamics and mechanics; 7260 Seismology: Theory and modeling; *KEYWORDS:* frictional sliding, surface roughness, oblique loading

Citation: Walsh, J. B., and Wenlu Zhu (2004), Sliding of a rough surface under oblique loading, *J. Geophys. Res.*, *109*, B05208, doi:10.1029/2004JB003027.

1. Introduction

[2] Earthquakes occur on faults, the nominally planar interfaces separating blocks loaded by tectonic forces oriented obliquely to the direction of slip. The blocks can be considered to be elastic, and the surfaces of the fault are rough. In the study reported here, we analyze the constitutive properties of this system, with the goal of relating displacement, applied stresses, changes in the components of energy, and the topography of the fault surfaces. This study is the latest in a series of studies to examine the constitutive behavior of rough surface under various loading conditions. The model we use was proposed by *Greenwood and Williamson* [1966] to analyze the closure between rough surfaces under normal stress. *Walsh* [2003] used Greenwood and Williamson's model in a study of sliding between rough surfaces under constant normal stress. In the analysis here, we analyze deformation of rough surfaces, again using Greenwood and Williamson's model, when both applied normal stress and shear stress are increased simultaneously. The present analysis will, in turn serve as the basis for projected investigations of the elastic and dissipative response of joints to dynamic loading and the deformation of joint networks.

[3] *Byerlee* [1966] was the first to examine the mechanics of earthquake generation experimentally, and his experiments were a direct simulation of the process we are studying theoretically. Byerlee, and many others since [see *Paterson*, 1978, and references therein] use the "triaxial" technique for their experimental studies of the frictional properties of rock surfaces. For these experiments, a cylinder of rock is cut on a plane at angle β to the axis. The sample is jacketed with an impermeable membrane, confining pressure p_0 is applied, and the axial load σ_1 is increased until slip occurs on the planar surface that divides the sample.

[4] Generally, slip on the planar surface is found by measuring the axial deformation of the sample, and calculating slip using the assumption that the surface is a smooth plane. The constitutive behavior of this system has a particularly simple form: as shown in Figure 1, no displacement occurs until the shear stress τ on the fault equals the frictional strength, $f\sigma$ (where f is the coefficient of friction, and σ is the normal stress on the slip plane). Real surfaces are not smooth, however. When two rough surfaces are pressed together, the normal stress acting on a contact between two relatively high asperities is greater than that for shorter ones. As shear stress is increased, slip starts at contacts with low contact stress, spreading to other more highly loaded contacts until the surface slides as a unit; the behavior is shown schematically in Figure 1.

[5] The precise description of the relationship between stress and displacement depends on the topography of the surface. Measurements of topography having considerable precision are now available [*Brown and Scholz*, 1986; *Boitnott et al.*, 1992]. The statistical analysis required to reduce these measurements to parameters—in particular, the areal density of asperities and the probability density distribution functions of asperity heights and tip radii—needed for a theoretical analysis of constitutive behavior has also been developed [*Cartwright and Longuet-Higgins*, 1956; *Longuet-Higgins*, 1957; *Nayak*, 1971]. Using these parameters, *Greenwood and Williamson* [1966] devised a simple model that they used to simulate the constitutive behavior of rough surfaces under normal stress. Their model employs a rough, elastic half-space in contact with a smooth half-space. The rough surface is a plane studded with

0148-0227/04/2004JB003027$09.00

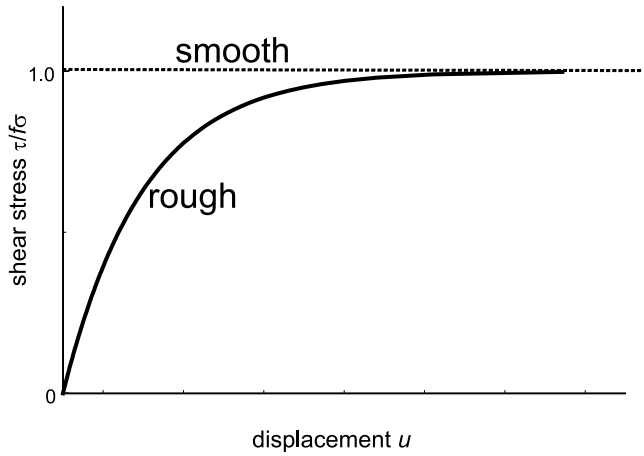

Figure 1. The relative slip u between two nominally planar surfaces under normal stress depends on the topology of the interface. Partial slip at the individual contacts between rough surfaces begins as shear stress is increased. Under higher applied shear stress, lightly loaded asperities slide as a unit when shear stress reaches the local contact "strength," $f\sigma_c$, where f is the friction coefficient and σ_c is the average normal stress on the contact. Displacement u increases further as slip spreads to more highly loaded asperities, until the surface slides as a unit at its frictional strength $f\sigma$. No preliminary slip occurs between perfectly smooth surfaces (an ideal situation, not attainable practically), and the transition from "stuck" to sliding is abrupt, as shown in the figure.

asperities having various heights h (Figure 2), defined by an arbitrary probability density distribution $g(h/\lambda)$ (where λ is a normalizing factor having the dimension of length). All asperities have the same tip radius R, and the spatial density n (number per unit area) is low enough that interaction between the deformation fields of neighbors is negligible. *Greenwood and Williamson* [1966] evaluated their expression for displacement between the two half spaces for two probability density distributions, Gaussian and the negative exponential $e^{-h/\lambda}$.

[6] *Brown and Scholz* [1986] used Greenwood and Williamson's model to analyze their measurements of the closure of rough rock surfaces under normal stress. Brown and Scholz calculated the theoretical response using Greenwood and Williamson's analysis, the probability density distribution $g(h/\lambda)$ having been determined empirically from their profilometer measurements. Data from measurements of closure between ground glass surfaces, ground surfaces of granite, quartzite, and marble samples, and of tension fractures in granite and quartzite samples compared favorably with their theoretical predictions.

[7] *Walsh* [2003] derived the theoretical constitutive relationship for slip under applied shear stress, the normal stress remaining constant, using *Greenwood and Williamson*'s [1966] model as the basis of his study. He found that the final form of the constitutive relationship was relatively insensitive to choice taken for the probability density function $g(h/\lambda)$ for asperity heights or for the radii of asperity tips; that is, uncertainties in experimental sliding data masked the differences between various theoretical constitutive relationships. In particular, Walsh found reasonable agreement between theory and experiment when he approximated the observed probability density distribution $g(h/\lambda)$ (which was represented by *Biegel et al.* [1992] as an inverted chi-squared distribution), by the simple negative exponential $e^{-h/\lambda}$ noted above. Comparison with data from sliding experiments carried out by *Biegel et al.* [1992] indicated that this approximation for the measured probability density distribution was adequate. Only a restricted range of asperity heights are involved in experiments carried out at confining pressures in the usual range of interest, and so a negative exponential generally will be satisfactory approximation, no matter what the actual $g(h/\lambda)$ may be.

[8] *Walsh* [2003] and *Greenwood and Williamson* [1966] assumed in their analysis that surface topography does not change during sliding and closure experiments. The real area of contact is small in both closure and sliding experiments and so contact stresses are high. One would expect damage to occur at highly stressed contacts, and indeed experimentalists often note that debris could be seen on the surfaces after sliding experiments. *Walsh* [2003] found good agreements between observed constitutive behavior and the behavior predicted by theory using topographical measurements made before the experiments were performed. Though changes in topography, undoubtedly occur, apparently the effect is small enough that it is lost in the various uncertainties inherent in even the most sophisticated sliding experiments now being carried out.

[9] In the analysis here, we extend *Walsh*'s [2003] analysis to the case where both normal and shear loads are increased. An example is the "triaxial" test [see, e.g., *Paterson*, 1978], in which the axial load is increased on cylindrical specimen cut into two parts by a cut at an angle to the axis; here, an increase in axial load causes increases in both the normal and shear stresses acting on the plane. As discussed above, the simplest description of the topography is good enough, and so we take *Greenwood and Williamson*'s [1966] representation of rough surfaces, with the probability density distribution $g(h/\lambda) = e^{-h/\lambda}$, as the basis of our analysis. Asperities are assumed to randomly distributed on the surface and separated from each other such that the effect of interaction is negligible. Deformation is elastic and local slip is opposed by Coulomb friction, with no time-dependent effects involved in either normal or shear responses. Only loading paths that cause monotonically increasing slip are consid-

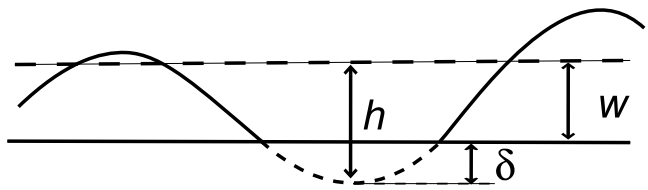

Figure 2. We simplify the analysis by considering slip between a rough surface and a smooth surface. The deformation at contacts is calculated following Hertz's procedure. As shown in the figure, shortening δ of an asperity is the difference between its height h and the separation w between the mid-plane of the topography and the smooth reference surface.

ered, and so instability at either the micro- and macro scale and the special treatment that must be introduced when the sense of shear is reversed can be ignored.

2. Analysis

2.1. Constitutive Behavior Under Normal Stress

[10] In *Greenwood and Williamson*'s [1966] model, all tip radii R have the same value and asperity heights h are distributed following the probability density distribution $g(h/\lambda)$ given by

$$g(h/\lambda) = e^{-h/\lambda}, \tag{1}$$

where λ is a characteristic length chosen to approximate the actual distribution found from topographical measurements. *Greenwood and Williamson* [1966], and later *Walsh* [2003], further simplified the problem by assuming that the rough surface rests on a planar surface, which without loss of generality, can be assumed to be rigid. Contacts between the surfaces are assumed to be so widely separated that each can be considered to act independently.

[11] Hertz's solution for the deformation at a contact between a sphere and a flat, rigid surface [see *Johnson*, 1987, chapter 4] forms the basis of the analysis, giving expressions relating the radius a of the contact circle, the deformation (h-w) of an asperity (see Figure 2) and the applied force p, as follows

$$a = \left[3pR\left(1-\nu^2\right)/4E\right]^{1/3} \tag{2a}$$

$$h - w = a^2/2R, \tag{2b}$$

where E and ν are Young's modulus and Possion's ratio, respectively. Combining equations (2a) and (2b), and rearranging gives an expression for the force p on an individual asperity, as follows:

$$p = \left[8E\sqrt{2R\lambda^3}/3\left(1-\nu^2\right)\right]\left(\frac{h-w}{\lambda}\right)^{3/2}. \tag{3}$$

Asperity heights are arranged according to the probability density distribution $g(h/\lambda)$ in equation (1). The total force P on a surface with N asperities is therefore

$$P = \left[8E\sqrt{2R\lambda^3}/3\left(1-\nu^2\right)\right]N\int_{w/\lambda}^{\infty}\left(\frac{h-w}{\lambda}\right)^{3/2}e^{-h/\lambda}d(h/\lambda). \tag{4}$$

Evaluating equation (4) gives an expression for the applied normal stress σ (=P per unit area), as follows:

$$\sigma = Se^{-w/\lambda}, \tag{5a}$$

where

$$S = 2nE\sqrt{2\pi R\lambda^3}/\left(1-\nu^2\right) \tag{5b}$$

and n is the number of asperities per unit area. Equations (5a) and (5b) and the development leading to them, are the same, except for notation, as those derived by *Greenwood and Williamson* [1966].

2.2. Constitutive Behavior in Shear

[12] The derivation of the relationship between applied shear stress τ and the resulting shear displacement u is analogous to that used by *Greenwood and Williams* [1966], which leads to equation (5). As described in section 2.1 on Greenwood and Williamson's model, we consider an elastic, rough surface in contact with a rigid smooth surface. Let us assume that the two surfaces are pressed together by a normal stress σ. The rigid platen is now advanced by shear displacement u. Some asperities are in contact with the platen, and these contacts are displaced elastically relative to the stationary rough surface. Other asperities are not in contact, because of non-interaction between contacts, these asperities are not affected by elastic deformation at surrounding contacts and so they remain stationary. *Mindlin and Deresiewicz* [1953] analyzed the deformation at the contact between two spheres under normal and shear forces p and t. They show that the circular area of contact is divided into two regions: an inner circle of radius c ($0 \le r \le c$) within which no slip occurs, surrounded by an annular area ($c \le r \le a$) where slip increases from zero at $r = c$ to a maximum at $r = a$. We use the convention that relative motion over part of a contact is defined as "slip," whereas "sliding" occurs when relative motion occurs over the contact as a unit. *Mindlin and Deresiewicz* [1953] found that the ratio c/a is determined uniquely (for monotonically increasing shear displacement u) by the expression [see *Johnson*, 1987]:

$$t/fp = 1 - (c/a)^3. \tag{6}$$

Further, they found that displacement u is related to applied shear force t by

$$u = \frac{3t(2-\nu)}{32G}\left(\frac{a^2-c^2}{a^3-c^3}\right), \tag{7}$$

where G is the shear modulus. We see in equation (7) that little slip occurs between the asperity and the platen when c/a is near unity. Part of the contact ($0 \le r \le c$) adheres to the platen until $c/a = 0$, when the contact slides as a unit. Combining equations (6) and (7) to remove c gives the constitutive relation for a single asperity as

$$t = fp\left\{1 - \left[1 - \frac{32}{3f}\left(\frac{G}{2-\nu}\right)\frac{a}{p}u\right]^{3/2}\right\}. \tag{8}$$

[13] *Mindlin and Deresiewicz* [1953] (in their Figure 7 and the accompanying text) show that equation (8) does not depend on the path followed to reach an arbitrary state (t, p, u). Their proof of the uniqueness of equation (8) consists of first choosing an arbitrary point on the (t, p, u) surface defined by equation (8); then a small normal force Δp (in our terminology) is superposed on the asperity, followed by superposing a small tangential force Δt, such that

$$\Delta t = f\Delta p. \tag{9}$$

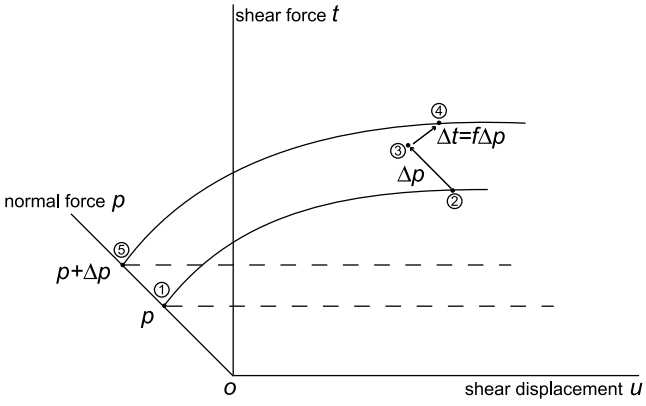

Figure 3. Each point on the (t, p, u) surface defines a unique state of stress acting on the contact. *Mindlin and Deresiewicz* [1953] considered an arbitrary point 2. At 2, normal force p is increased by Δp and then shear force t is increased by $f\Delta p$ to arrive at 4. *Mindlin and Deresiewicz* [1953] show that the state of stress at 4 is the same that would be obtained by following path o–1–5–4, when normal force at 1 where shear force is zero is increased by Δp to 5 and then shear force is increased by $t + f\Delta p$ to 4.

This stress path is shown schematically in Figure 3 as o–1–2–3–4. *Mindlin and Deresiewicz* [1953] then chose another path, where the superposed Δp is applied at the point (0, p, 0), and following the path o–1–5–4 in Figure 3, shear force t is increased at constant normal force ($p + \Delta p$) to the same point ($t + f\Delta p$, $p + \Delta p$, $u + \Delta u$) reached using prior stress path. *Mindlin and Deresiewicz* [1953] show that the stress distribution on the contact at 4 is the same, independent of the path used.

[14] Using the same reasoning, one can show for rough surfaces that the stress state at all contacts does not depend on the path chosen to reach an arbitrary point (τ, σ, u) on the surface (e.g., Figure 4) which defines allowable states for which slip and sliding can occur. *Mindlin and Deresiewicz* [1953, equation (4)] show that the compliance dw_k/dp_k under normal force for an arbitrary asperity k on the rough surface is given by

$$dw_k/dp_k = (1 - \upsilon)/4Ga_k \tag{10a}$$

and the compliance du_k/dt_k (*Mindlin and Deresiewicz* [1953], section 7) under shear force for the path 2–3–4 is

$$du_k/dt_k = (2 - \upsilon)/8Ga_k, \tag{10b}$$

where a_k is the radius of the contact k.

[15] Now consider a rough surface having a family of N asperities; we use differential changes in the variables because, in general, curved shear paths may be considered. First, a normal displacement dw, and then a shear displacement du, is applied to the rough surface, such that

$$dw/du = dw_k/du_k = 2(1 - \upsilon)/f(2 - \upsilon). \tag{11}$$

From equations (10) and (11), we find that the ratio dt_k/dp_k is given by

$$dt_k/dp_k = f. \tag{12}$$

[16] We see in equation (10) that the changes in forces acting on a contact depends on its radius, which in general is not the same for all asperities. Though the change in force is not the same for all asperities, we see in equation (12) that the ratio is the same; that is, every contact goes through the stress/deformation history (o–1–2–3–4) prescribed by *Mindlin and Deresiewicz* [1953] in Figure 3. Therefore the rough surface as a body can also reach state 4 following path o–1–5–4. Each point on the surface (τ, σ, u) defines a unique state for all contacts on the surface, in analogy with *Mindlin and Deresiewicz*'s [1953] results.

[17] One difference between the analysis here and that developed by *Mindlin and Deresiewicz* [1953] is that increasing the normal stress acting on a rough surface not only increases the area of existing contacts but also increases the number of contacts. The total number of contacts is N, and so increasing normal stress by $d\sigma_1$ increases the number of contacts by dN_1 and the force "on" each new contact has increased from zero to dp_1. Increasing shear force as in step 3–4 means that each new asperity has reached its "frictional strength," and will slide as a unit under further increases in shear load.

[18] Now consider the path o–1–5 in Figure 3. In step 1–5, the number of asperities is increased by dN_1 and the normal force on each is dp_1, the same values found in step 2–3. When shear stress is increased in step 5–4, these new asperities slide as units once the shear force attains the value $f dp_1$, and they stay in this condition under further increases in shear. We see that the state at 4 of new contacts, as well as the existing ones, is the same independent of the path taken.

[19] To sum the contribution of individual contacts, we first express the shear force t, the normal force p and contact radius a in equation (8) can be expressed in terms of the deformation (h-w) of the asperity; using equations (2a) and (2b) in equation (8) gives

$$t/f = \frac{8E\sqrt{2R\lambda^3}}{3(1-\nu^2)}\left\{\left(\frac{h-w}{\lambda}\right)^{3/2} - \left[\frac{h-w}{\lambda} - \frac{2u(1-\nu)}{f\lambda(2-\nu)}\right]^{3/2}\right\}. \tag{13}$$

Summing the contributions of individual asperities over a population defined by the probability density distribution

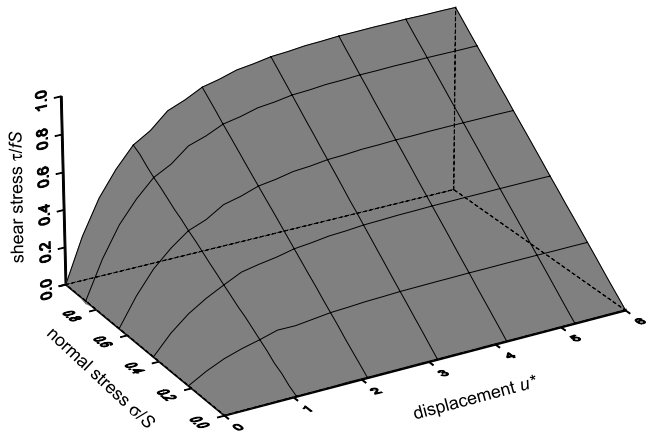

Figure 4. The surface defined by equations (15a) and (15b) in the text where stresses τ and σ have been nondimensionalized using the modified stiffness S given by (5b).

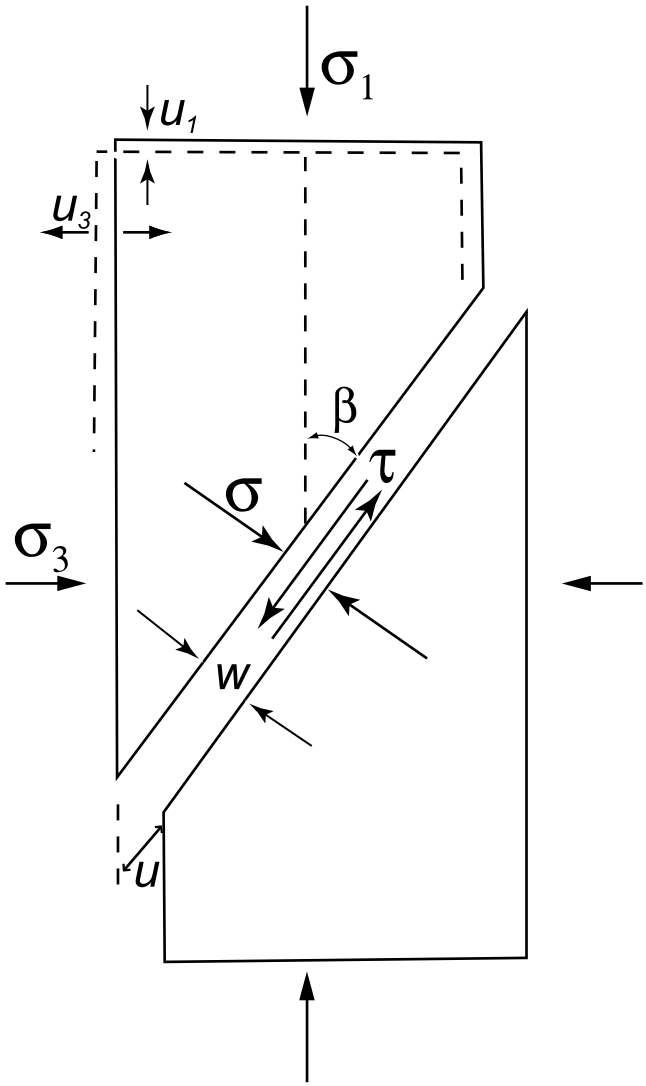

Figure 5. The configuration of a sample used in typical triaxial tests is a cylinder cut by a plane oriented at an angle β to the axis. Applied stresses σ_1 and σ_3 produce normal stress σ and shear stress τ on the interface: The relationship between these components is given by equations (16a) and (16b) for the case where σ_3 has the constant value p_0. The axial and radial displacements u_1 and u_3 are related to the normal and shear displacements w and u at the interface by equation (20).

$g(h/\lambda)$ of asperity heights given here by equation (1), we find that the constitutive relation is given by

$$\tau = fS\int_{w/\lambda}^{\infty}\left\{\left(\frac{h-w}{\lambda}\right)^{3/2}-\left[\frac{h-w}{\lambda}-\frac{2u(1-\nu)}{f\lambda(2-\nu)}\right]^{3/2}\right\}e^{-h/\lambda}d(h/\lambda). \tag{14}$$

Note equation (14) is derived for the case where normal stress is constant. In equation (14), both the applied shear load and the frictional resistance at contacts are applied at the rough surface, and so no elastic deformation of the elastic body is involved. Evaluating equation (14) and introducing equation (4) for the normal stress σ, we find

$$\tau = f\sigma\left(1-e^{-u^*}\right), \tag{15a}$$

where the nondimensional displacement u^* is

$$u^* = (u/f\lambda)\frac{2(1-\nu)}{2-\nu}. \tag{15b}$$

The surface representing equation (15a) is plotted in nondimensional form in Figure 4. As we noted after (8) for the case of a single asperity, different paths can be used to arrive at some equilibrium state (τ, σ, u^*), but having reached it, τ, σ, u^* are uniquely related by equation (15).

2.3. Triaxial Tests

[20] The samples used in triaxial experiments are cylinders cut by a plane at an angle β to the axis, as in Figure 5. In an experiment, confining pressure p_0 ($p_0 = \sigma_3$) is applied, and then the axial load σ_1 is increase from p_0 while axial displacement u_1, is monitored. Using Mohr's construction, we find that the change $\Delta\sigma$ in normal stress σ and in shear stress τ acting on the plane are given by

$$\begin{aligned}\Delta\sigma &= \Delta\sigma_1\sin^2\beta\\ \tau &= \Delta\sigma_1\sin\beta\cos\beta\end{aligned} \tag{16a}$$

where differential stresses $\Delta\sigma$ and $\Delta\sigma_1$ are

$$\begin{aligned}\Delta\sigma_1 &= \sigma_1 - p_0\\ \Delta\sigma &= \sigma - p_0.\end{aligned} \tag{16b}$$

The constitutive behavior in terms of (τ, σ, u) refer to the slip plane as in Figure 4 is found from equations (15) and (16), in the form

$$\tau/fp_0 = (\sigma/p_0)\left(1-e^{-u^*}\right), \tag{17a}$$

where the path is defined by the relationship

$$\begin{aligned}\tau/p_0 &= (\Delta\sigma/p_0)\cot\beta\\ &= (\sigma/p_0 - 1)\cot\beta.\end{aligned} \tag{17b}$$

The surface defined by equation (17), with deformation paths for planes at several angles β, is given in Figure 6.

[21] Note that not all deformation paths on the surface are permissible. In the first place, *Mindlin and Deresiewicz*'s [1953] analysis on which equation (17) is based is valid only for cases where deformation u increases monotonically with increasing shear stress τ. *Mindlin and Deresiewicz* [1953] also show [see *Johnson*, 1987, chapter 7.3] that slip cannot occur unless

$$d\tau/d\sigma \geq f. \tag{18}$$

Introducing equation (17b), equation (18) becomes

$$\begin{aligned}\tau/f\Delta\sigma = \cot\beta/f &\geq 1\\ f\tan\beta &\leq 1.\end{aligned} \tag{19}$$

The restriction in equation (19) is shown graphically in Figure 6. Also shown in Figure 6 is the restriction that shear

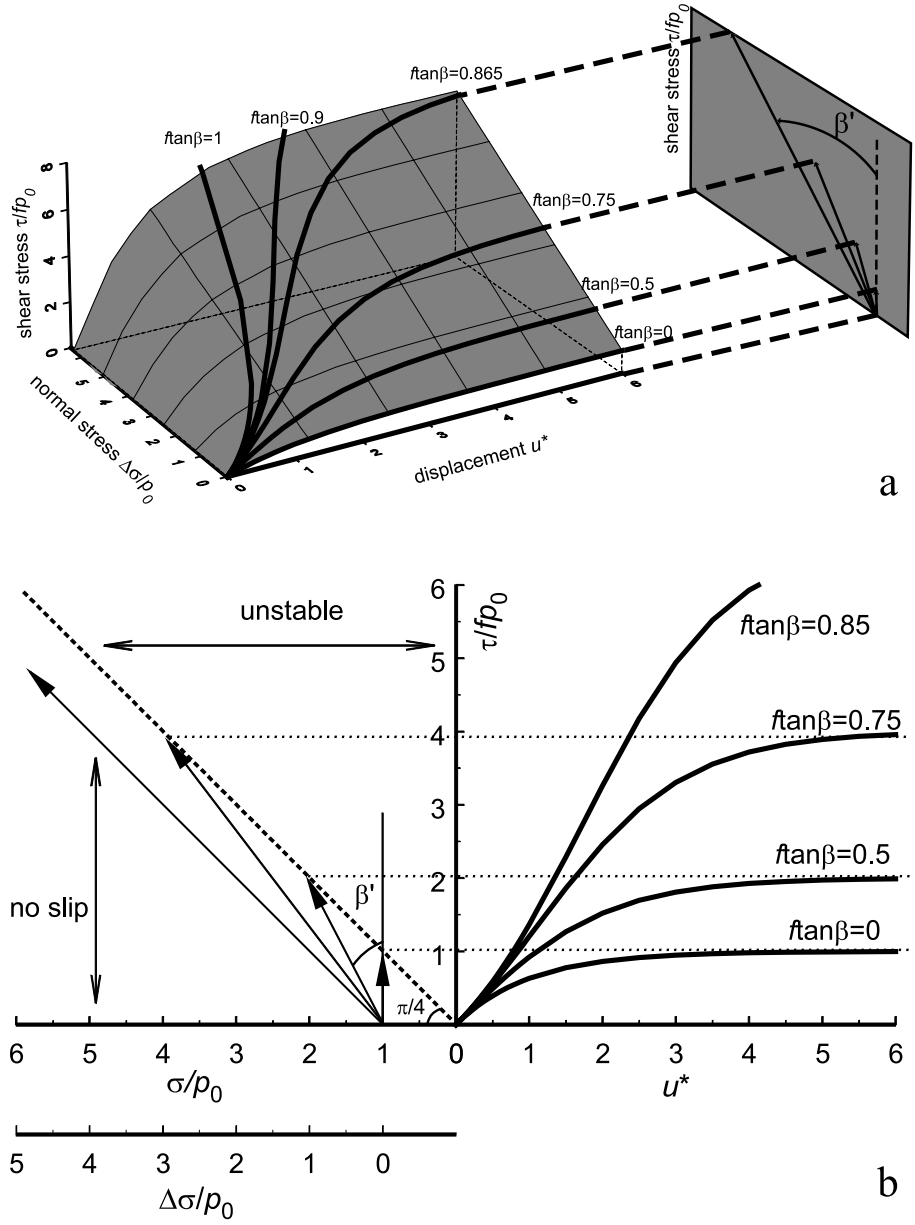

Figure 6. (a) The shear stress τ/fp_0, normal stress $\Delta\sigma_1/p_0$, and shear displacement u^* (each appropriately nondimensionalized) for triaxial experiments on samples having saw cuts at angle β to the axis with friction coefficient f. The trace of these paths on the shear stress-normal stress plane are straight lines making an angle β' with the vertical axis, where $\tan\beta' = (1/f)\tan\beta$. (b) The same information in Figure 6a is replotted here to show more clearly permissible stress-displacement paths. The region marked "unstable" lies above the "yield" surface in this figure, where applied shear is greater than the frictional strength of the surface. Saw cuts in the region marked "no slip" remain locked under increasing axial normal stress because the requirement given by equation (15) is violated, that is, because the frictional strength of the joint increases faster than the applied shear stress.

stress τ on the saw cut cannot exceed the frictional strength, i.e.,

$$\tau/f\sigma \le 1. \tag{20}$$

[22] The constitutive behavior can also be expressed in terms of the applied axial stress σ_1, introducing (20) into equations (19) and (5), we find

$$e^{-u^*} = \left[\frac{1-(\Delta\sigma_1/p_0)\sin^2\beta(\cot\beta/f-1)}{1+(\Delta\sigma_1/p_0)\sin^2\beta}\right] \qquad e^{\Delta w/\lambda} = 1+(\Delta\sigma_1/p_0)\sin^2\beta. \tag{21}$$

Note in equation (21) that the nondimensional displacement u^* is given, to a reasonable approximation, by

$$u^* \approx u/f\lambda. \tag{22}$$

We see in equation (15b) that equation (8) is exact for $\nu = 0$, and the discrepancy is only 14% for $\nu = 0.25$. Displacements u and Δw in equation (21) now take the form

$$u/\lambda = f\ln\left[\frac{1+(\Delta\sigma_1/p_0)\sin^2\beta}{1-(\Delta\sigma_1/p_0)\sin^2\beta(\cot\beta-f)/f}\right] \qquad \Delta w/\lambda = \ln\left[1+(\Delta\sigma_1/p_0)\sin^2\beta\right]. \tag{23}$$

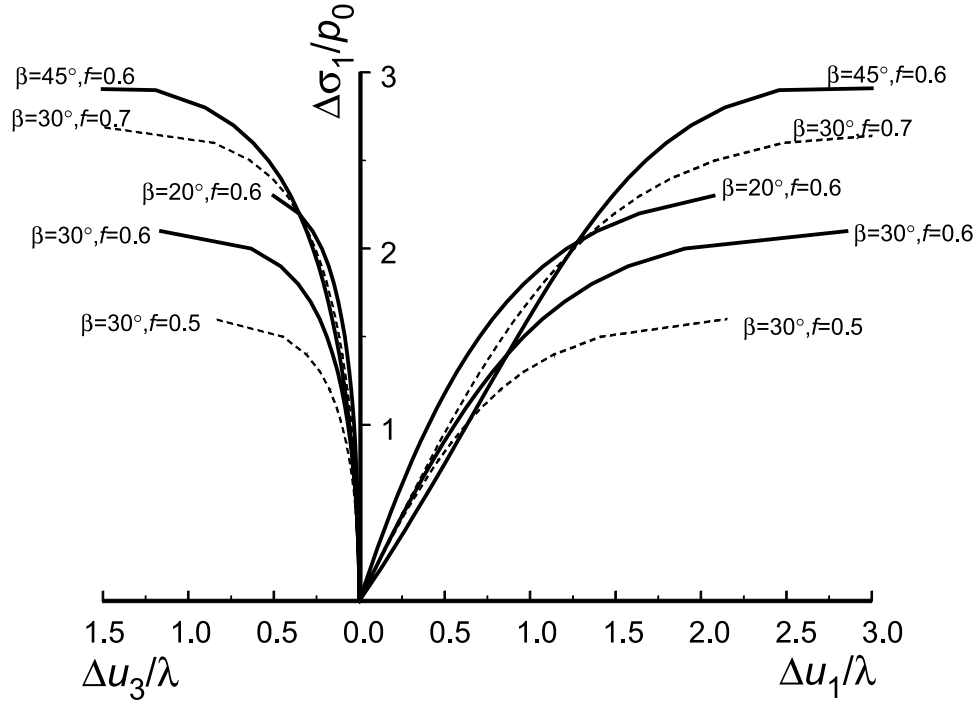

Figure 7. Axial displacement $\Delta u_1/\lambda$ and radial displacement $\Delta u_3/\lambda$ as a function of applied axial normal stress $\Delta\sigma_1/p_0$ for saw cuts having friction coefficient f oriented at angle β to the axis of sample. All curves in this figure reach an asymptotic value at large values of Δu_1.

The relationship between the axial load $\Delta\sigma_1$ and displacements on the saw cut is illustrated in Figure 7 for values of β and f in the range most prevalent in triaxial experiments.

[23] Slip displacement u along the saw cut is commonly calculated assuming that closure Δw normal to the saw cut is zero. To evaluate the accuracy of this assumption, we first relate displacements (Δu_1, Δu_3) to (u, Δw) following a straightforward geometrical calculation:

$$\begin{aligned} \Delta u_1 &= u\cos\beta + \Delta w\sin\beta \\ \Delta u_3 &= u\sin\beta - \Delta w\cos\beta. \end{aligned} \tag{24}$$

For $\Delta w = 0$, equation (24) gives the approximate value u_A for slip as

$$u_A = \Delta u_1/\cos\beta. \tag{25}$$

From equations (24) and (25), the relative error ε in the approximation is

$$\varepsilon = (u_A - u)/u = \Delta w\tan\beta/u. \tag{26}$$

An expression for ε valid over the full range of values for $\Delta\sigma_1/p_0$ could be derived, but here approximations at small $\Delta\sigma_1/p_0$ and at large $\Delta\sigma_1/p_0$ are adequate. We find that the error for values of $\Delta\sigma_1/p_0$ such that $(\Delta\sigma_1/p_0)\sin^2\beta \ll 1$, is approximately

$$\varepsilon \approx \tan\beta, \tag{27}$$

and the error when $(\Delta\sigma_1/p_0)\sin^2\beta$ approaches the maximum value is approximately zero. We see that neglecting closure in a triaxial experiment causes a negligible increase in the error in slip except in the early stages of deformation. These early stages are not important in experiments where sliding between rough surfaces is being studied; however, this stage of the constitutive behavior contains information about the rough surface itself and deformation at individual contacts that is vital in studies, for example, of stick slip and behavior when both surfaces are rough.

3. Discussion

[24] We have presented a theoretical analysis of slip between rough, elastic surfaces caused by tractions oriented obliquely to the plane of the interface. We were unable to compare our theoretical results with experimental data; although many studies of fault deformation in triaxial experiments can be found in the literature, the measurements of slip and closure were not sufficiently precise for our purpose. *Walsh* [2003] developed theory for the special case where normal stress acting on the fault remains constant. The good agreement he found between his results and data from rotary shear experiments gives us confidence that our theoretical results have an adequate experimental basis. The analysis is an extension of *Greenwood and Williamson*'s [1966] work on closure of rough surfaces under normal stress and relies on *Walsh*'s [2003] study of slip under applied shear and constant normal stress. Walsh showed that a reasonably accurate representation of the constitutive behavior observed experimentally can be obtained from simple (statistically speaking) simulations of the topography of rough surfaces, and so we chose a very simple model here, namely, a rough surface composed of asperities, all having the same tip radius R, with heights h having a probability density distribution $g(h/\lambda)$ given by the negative exponential $e^{-h/\lambda}$ (see equation (1)). The

asperities are distributed on an elastic half-space and all in contact with a rigid, smooth surface.

[25] First, the surfaces are pressed together under normal stress σ, causing normal displacement w, as given by (5). *Cattaneo* [1938] and, independently, *Mindlin* [1949] [see also *Mindlin and Deresiewicz*, 1953] showed that the superposition of shear stress causes partial slip at the contact, starting at the edge and progressing radially (for asperities with spherical tips) inward as shear stress is increased. Eventually the frictional strength of the contact is reached and the asperity slides under constant shear. As shown in the text, partial slip for a rough surface begins when shear stress is applied, as in the case of an individual asperity. The frictional strength is first reached at lightly loaded contacts, then spreading to contacts under higher normal stress until the rough surface slides as a body. The theoretical constitutive behavior derived in the text for this process is given by equations (15a) and (15b) and the surface defined by the constitutive equation is shown in Figure 4.

[26] Note in equation (15) that displacement is measured in units of λ, the length parameter which defines the probability density distribution $g(h/\lambda)$ of asperity heights. Here we chose the negative exponential $e^{-h/\lambda}$ to represent the distribution. Therefore distributions having small values of λ have a broad range of heights in the population. Asperity heights derived from measurements of surface topography have been represented as having a Gaussian distribution [*Greenwood and Williamson*, 1966] and an inverted chi-square distribution [*Adler and Firman*, 1981; *Brown and Scholz*, 1986; *Yoshioka and Scholz*, 1989; *Biegel et al.*, 1992]. The negative exponential $e^{-h/\lambda}$ used here is an approximation to these more exact distributions. *Walsh* [2003] shows that the approximation is adequate for representing both normal and shear constitutive behavior because the range of asperity heights involved in typical applications is small.

[27] The contact at an individual asperity loaded by a force oblique to its axis experiences both an increase in normal stress and proportional increase in the shear component. Therefore the radius of the contact increases and concurrently the annular region of slip progresses radially inward. Clearly, for angles that the normal component is sufficiently greater, proportionally, than the shear component, the increase in contact radius overwhelms the radial growth of the annulus of slip, and no slip occurs. *Mindlin and Deresiewicz* [1953] show that no partial slip occurs for angles β (see Figure 5) and friction coefficient f such that $f\tan\beta \geq 1$. Slip at each contact on a rough surface is subject to the same restriction, and so sliding occurs only for a range of oblique loadings; these are illustrated in Figures 6a and 6b.

[28] The triaxial test is one of several techniques used to measure the frictional properties of rock surfaces experimentally [see *Paterson*, 1978]. The sample configuration is described in Figure 5. The constitutive behavior in terms of stresses ($\Delta\sigma_1$, $\Delta\sigma_3$) and displacements (Δu_1, Δu_3) referred to the axial and radial coordinates of the sample is given by equations (23) and (24) and is shown graphically in Figure 7. Note in the figure that the slope $d(\Delta\sigma_1/p_0)/d(\Delta u_3/\lambda)$ of the stress-lateral strain curve is infinity near the origin, whereas the slope $d(\Delta\sigma_1/p_0)/d(\Delta u_1/\lambda)$ depends on the angle β but not on the friction coefficient. Analysis of equations (23) and (24) for $(\Delta\sigma_1/p_0) \ll 1$ shows that, at the origin,

$$\begin{aligned} d(\Delta\sigma_1/p_0)/d(\Delta u_1/\lambda) &= \sin^2\beta \\ d(\Delta\sigma_1/p_0)/d(\Delta u_3/\lambda) &= 0. \end{aligned} \tag{28}$$

Likewise, we find from equation (23) that the maximum value $(\Delta\sigma_1/p_0)_M$ of $(\Delta\sigma_1/p_0)$ depends on both β and f; that is

$$(\Delta\sigma_1/p_0)_M = f/(\sin\beta\cos\beta)(1 - f\tan\beta), \tag{29}$$

where, as discussed above, $f\tan\beta \leq 1$.

[29] In triaxial tests, only axial displacement Δu, is measured and slip displacement u is estimated by assuming that closure $\Delta w = 0$. The approximate value u_A of slip u calculated using this procedure is $\Delta u_1/\cos\beta$. As shown by equation (25), the error ε involved in making this approximation, defined by the relation $\varepsilon = (u_A - u)/u$, is found to be equal to $\tan\beta$ at low values of $\Delta\sigma_1/p_0$, and it approaches zero as $\Delta\sigma_1/p_0$ approached its maximum value.

[30] We have analyzed here only the case where applied shear stress and slip increase monotonically, with the qualification that changes in the shear and normal components of stress do not violate the requirement that $d\tau/d\sigma = \cot\beta \geq f$. These conditions limit stress deformation paths to the "yield" surface in Figure 4. Other paths are, of course, possible, but the analysis here would have to be extended to define their properties. *Olsson*'s [1987] experimental study of the effects of changes in normal stress on friction serves as an example of load paths where stresses increase monotonically, but the requirement of $d\tau/d\sigma \geq f$ is violated. In Olsson's friction experiments, the shear stress for slip increased under constant normal stress ($d\tau/d\sigma \geq f$); the normal stress was then increased, as shear stress remaining constant ($d\tau/d\sigma = 0$); then shear stress was increased and slip was resumed under the new normal stress ($d\tau/d\sigma \geq f$). For the segment where normal stress was increased, our analysis isn't applicable until shear stress has increased sufficiently that the path again intersects the yield surface. Further slip follows the deformation path on the surface which would have been traced had the experiment been started at that normal stress.

[31] **Acknowledgments.** J. B. Walsh was supported by grant EAR-9903217 from the National Science Foundation. W. Zhu gratefully acknowledges the support of the Department of Energy through grant DE-FG02-00ER15058 and WHOI Mellon Independent Study Award (2000). We thank A. McGarr and Y. Bernabé for their penetrating and convincing reviews.

References

Adler, R. J., and D. Firman (1981), A non-Gaussian model for random surfaces, *Philos. Trans. R. Soc. London, Ser. A*, *303*, 433–452.

Biegel, R. L., W. Wang, C. H. Scholz, and N. Yoshioka (1992), Micromechanics of rock friction: 1. Effects of surface roughness on initial friction and slip hardening in Westerly granite, *J. Geophys. Res.*, *97*, 8951–8964.

Boitnott, G. N., R. L. Biegel, C. H. Scholz, N. Yoshioka, and W. Wang (1992), Micromechanics of rock friction: 2. Quantitative modeling of initial friction with contact theory, *J. Geophys. Res.*, *97*, 8965–8978.

Brown, S. R., and C. H. Scholz (1986), Closure of rock joints, *J. Geophys. Res.*, *91*, 4939–4998.

Byerlee, J. D. (1966), The frictional characteristics of westerly granite, Ph.D. thesis, Mass. Inst. of Technol., Cambridge.

Cartwright, D. E., and M. S. Longuet-Higgins (1956), The statistical distribution of the maxima of a random function, *Proc. R. Soc. London*, *Ser. A*, *237*, 212–232.

Cattaneo, C. (1938), Sul contatto di due corpi elastici: Distributzione locale degli sforzi, *Rend. Accad. Naz. Lincei*, *27*(6), 342, 434, 474.

Greenwood, J. A., and J. B. P. Williamson (1966), Contact of nominally flat surface, *Proc. R. Soc. London*, *Ser. A*, *295*, 300–319.

Johnson, K. L. (1987), *Contact Mechanics*, Cambridge Univ. Press, New York.

Longuet-Higgins, M. S. (1957), The statistical analysis of a random moving surface, *Philos. Trans. R. Soc. London*, *Ser. A*, *249*, 321–387.

Mindlin, R. D. (1949), Compliance of elastic bodies in contact, *Trans. ASME, Ser. E, J. Appl. Mech.*, *16*, 259.

Mindlin, R. D., and H. Deresiewicz (1953), Elastic spheres in contact under varying oblique forces, *J. Appl. Mech.*, *16*, 259–268.

Nayak, P. R. (1971), Random process model of rough surfaces, *J. Lubr. Technol.*, *93*, 398–407.

Olssen, W. A. (1987), The effects of changes in normal stress on rock friction, in *Constitutive Laws for Engineering Materials: Theory and Applications*, edited by C. S. Desai et al., Elsevier Sci., New York.

Paterson, M. S. (1978), *Experimental Rock Deformation: The Brittle Field*, Springer-Verlag, New York.

Walsh, J. B. (2003), A theoretical analysis of sliding of rough surfaces, *J. Geophys. Res.*, *108*(B8), 2385, doi:10.1029/2002JB002127.

Yoshioka, N., and C. H. Scholz (1989), Elastic properties of contacting surfaces under normal and shear loads: 1. Theory, *J. Geophys. Res.*, *94*, 17,681–17,690.

J. B. Walsh, Box 22, Adamsville, RI 02801, USA. (jwalsh1373@aol.com)

W. Zhu, Department of Geology and Geophysics, Woods Hole Oceanographic Institution, Woods Hole, MA 02543, USA. (wzhu@whoi.edu)